GEOLOGY | THE GEOLOGICAL SOCIETY OF AMERICA®

https://doi.org/10.1130/G45812.1

Manuscript received 13 June 2018
Revised manuscript received 7 January 2019
Manuscript accepted 11 January 2019

Coupled carbon and silica cycle perturbations during the Marinoan snowball Earth deglaciation

Donald E. Penman and Alan D. Rooney
Department of Geology and Geophysics, Yale University, New Haven, Connecticut 06520, USA

ABSTRACT

The snowball Earth hypothesis proposes that if polar ice sheets were to advance equatorward of a mid-latitude threshold, runaway ice-albedo effects would lead to a stable, globally ice-covered climate state that would require extremely high atmospheric pCO_2 levels (supplied by volcanic degassing over millions of years) for deglaciation. Geologic evidence, including globally distributed and low-latitude glacial deposits, suggests that two such global glaciations occurred during the Neoproterozoic. We model the coupled carbon and silica cycles through a snowball Earth event, including the extremely high pCO_2 and dramatically accelerated chemical weathering of its aftermath. The enhanced delivery of dissolved weathering products to the ocean induces elevated sedimentary burial of $CaCO_3$ (deposited as "cap carbonates") and SiO_2. Uncertainty in the relative importance of carbonate versus silicate weathering allows a wide range of possible $CaCO_3$ burial magnitude, potentially dwarfing that of SiO_2. However, total SiO_2 burial is insensitive to weathering strengths, and is set by the amount of CO_2 required for deglaciation (~10^{19} mol). Chert associated with Marinoan post-glacial cap carbonates in Africa and Mongolia corroborate modeled predictions of elevated SiO_2 burial.

INTRODUCTION

Synchronous, globally distributed, low-latitude glacial deposits (Evans and Raub, 2011; Kirschvink, 1992) suggest that near-global glaciation occurred at least twice (the Marinoan and Sturtian glaciations) in the Neoproterozoic. The snowball Earth (SE) hypothesis (Hoffman et al., 1998; Kirschvink, 1992) attributes such glaciations to the equatorward advance of polar ice sheets across a mid-latitudinal threshold, beyond which runaway ice-albedo effects led to a stable, globally glaciated Earth (see Hoffman et al. [2017] for a summary of SE events). The high-albedo, low-temperature SE climate state would require extremely high atmospheric pCO_2 (Caldeira and Kasting, 1992; Le Hir et al., 2008b), supplied by volcanic degassing in the absence of silicate weathering (Si-weathering) for millions of years, for deglaciation (Walker et al., 1981). The high pCO_2 required to overcome a SE state (~0.12 bar [Caldeira and Kasting, 1992] or higher [Pierrehumbert, 2004]) would significantly accelerate the rate of continental chemical weathering (Berner et al., 1983; Walker et al., 1981) following deglaciation.

The Marinoan and Sturtian cap sequences are distinct, but both likely formed in stratified water masses during intervals of enhanced chemical weathering in the high-pCO_2 SE aftermath (Higgins and Schrag, 2003; Rooney et al., 2014; Yang et al., 2017). Ca and Mg isotopes (Huang et al., 2016; Kasemann et al., 2014) support elevated chemical weathering rates of both silicates and carbonates due to high pCO_2 (Bao et al., 2008) following the Marinoan, while Os and Sr isotopes support elevated post-Sturtian weathering (Rooney et al., 2014).

Elevated weathering would enhance the delivery of weathering products (dissolved silicate [DSi], dissolved inorganic carbon [DIC], and cations, which contribute alkalinity) to the oceans via the generalized reactions (Urey, 1952):

$$CaCO_3 + CO_2 + H_2O \rightarrow 2HCO_3^- + Ca^{2+}; \quad (1)$$

$$CaSiO_3 + 2CO_2 + 3H_2O \rightarrow 2HCO_3^- + H_4SiO_4 + Ca^{2+}. \quad (2)$$

The addition of alkalinity and DIC to seawater in the above 1:1 ratio (the products of Reactions 1 and 2) elevates the saturation state of carbonate (Ω), favoring its precipitation and burial in sediments:

$$2HCO_3^- + Ca^{2+} \rightarrow CaCO_3 + CO_2 + H_2O\ . \quad (3)$$

Widespread evidence for significantly elevated post-SE carbonate burial comes in the form of "cap carbonates," globally ubiquitous 10-m-scale layers of calcite and dolomite overlying glaciogenic deposits and glaciated surfaces (Hoffman et al., 2007; Hoffman and Schrag, 2002) with sedimentological features indicating rapid, inorganic precipitation (James et al., 2001). The elevated DSi flux from (from Equation 2) should also promote the precipitation and burial of SiO_2:

$$H_4SiO_4 \rightarrow SiO_2 + 2H_2O\ , \quad (4)$$

which in the Precambrian was accomplished by inorganic precipitation of cristobalite, tridymite, or microcrystalline quartz and preserved in sediments as their diagenetic product, chert (Maliva et al., 1989; Siever, 1992). While the link between elevated post-SE weathering and cap carbonates is established (Higgins and Schrag, 2003; Hoffman and Schrag, 2002), the effects on the ocean's Si cycle and any connection to SiO_2 burial has received little attention.

MODELING POST-SNOWBALL WEATHERING

To explore the geochemical implications of elevated chemical weathering during SE deglaciation, we perform a suite of simulations using a model of the coupled Precambrian C and Si cycles (PreCOSCIOUS, the PreCambrian Ocean Silica Carbon Inorganic Ocean Underwater Sediment model, described in the GSA Data Repository[1] and in Figure 1), constructed for this purpose by combining elements of previous models. PreCOSCIOUS uses the three-box architecture (atmosphere, shallow ocean, and deep ocean) of previous SE geochemical models (Higgins and Schrag, 2003; Le Hir et al., 2008b). Carbonate chemistry and weathering feedbacks are adapted from the carbon cycle model LOSCAR (Zeebe, 2012), and a Si cycle was modified from Penman (2016) to include the

[1]GSA Data Repository item 2019107, detailed description of the PreCOSCIOUS model, snowball Earth sensitivity experiments, and MATLAB code for reproducing the runs described in the text, is available online at http://www.geosociety.org/datarepository/2019/, or on request from editing@geosociety.org.

CITATION: Penman, D.E., and Rooney, A.D., 2019, Coupled carbon and silica cycle perturbations during the Marinoan snowball Earth deglaciation: Geology, https://doi.org/10.1130/G45812.1

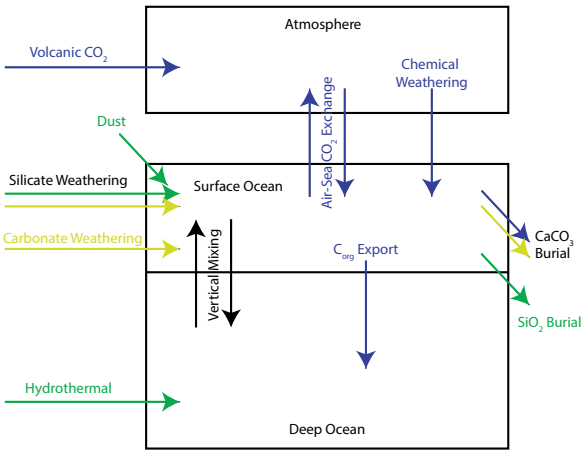

Figure 1. PreCOSCIOUS (PreCambrian Ocean Silica Carbon Inorganic Ocean Underwater Sediment model; see the Data Repository [see footnote 1]) architecture of reservoirs and fluxes. Fluxes are color-coded by tracer: green represents dissolved silica fluxes, yellow represents alkalinity, and blue represents carbon (C_{org}—organic carbon). Black represents combination of tracers.

Precambrian abiotic SiO_2 precipitation (Maliva et al., 1989; Siever, 1992). Technical details (equations, constants, references, and MATLAB code) are included in the Data Repository.

For each time step (~0.01 yr), input and output fluxes of four tracers in each reservoir are calculated: carbon (atmospheric CO_2 and seawater DIC), alkalinity, Ca^{2+}, and DSi. The atmospheric CO_2 budget includes volcanogenic input, removal by carbonate and Si-weathering fluxes, (Equations 1 and 2, the rates of which are functions of pCO_2 after Walker and Kasting [1992] and scaled to modern fluxes), and air-sea gas exchange with the surface ocean based on the degree of pCO_2 disequilibrium (after Zeebe, 2012). pCO_2 determines temperatures (using a simple climate sensitivity with a decay function, after Zeebe [2012]), which affect the equilibrium constants used to calculate full seawater carbonate chemistry from [DIC] and total alkalinity (TA). The dissolved products of chemical weathering (DIC, DSi, and TA) are delivered to the surface ocean, where they fuel precipitation and burial of $CaCO_3$ (at a rate governed by Ω) and SiO_2 (governed by [DSi]) from the surface ocean, consistent with Precambrian modes of SiO_2 (Maliva et al., 1989; Siever, 1992) and $CaCO_3$ (Zeebe and Westbroek, 2003) burial. Both $CaCO_3$ and SiO_2 precipitation occur only above a critical threshold of oversaturation, resulting in a "Strangelove ocean" (Zeebe and Westbroek, 2003) with very high Ω and [DSi]. The surface and deep oceans are linked by vertical mixing applied to all tracers, and by a DIC flux from the surface to deep representing the formation, sinking, and remineralization of organic carbon. Before experiments, the model was run for millions of model years until it reached a stable equilibrium, characterized by constant concentrations of all tracers in all reservoirs, carbon input by volcanic degassing perfectly balanced by Si-weathering and $CaCO_3$ burial.

A simple SE forcing halts carbonate and Si-weathering and organic carbon export and sets ocean temperatures to 0 °C. A complete SE experiment is shown in Figure 2, using a favored set of constants and boundary conditions (default run). Sensitivity tests to explore different configurations are detailed in the Data Repository. When the SE forcing is applied, the supply of weathering-derived alkalinity to fuel carbonate burial is shut off, and subsequently DIC removal quickly ceases and CO_2 begins to accumulate in the atmosphere at ~18,000 ppm/m.y. Dissolution of $CaCO_3$ (delivered by physical erosion and transport by glacial action; Hoffman and Schrag, 2002) also occurs whenever $\Omega < 1$, which maintains carbonate saturation and imparts an increase in seawater $[Ca^{2+}]$ during glaciation. The importance of $[Ca^{2+}]$ rise for Ω and sensitivity tests that omit this feature are explored in the Data Repository. DSi inputs are significantly reduced without Si-weathering, but hydrothermal DSi input continues and the Si-cycle reaches a stable state with lower [DSi] and SiO_2 burial rate. The default run takes ~6.7 m.y. for pCO_2 to reach the 0.12 bar deglaciation threshold (used in the default run for consistency with previous SE modeling, e.g., Higgins and Schrag, 2003; higher thresholds are explored in the Data Repository). Using different configurations (detailed in the Data Repository), the SE duration ranges from 5 to 16 m.y., in agreement with the 5–14 m.y. duration of the Marinoan glaciation suggested by geochronology (Hoffman et al., 2017).

Upon deglaciation, the surface rapidly warms due to high pCO_2 from 0 to ~35 °C and weathering rates immediately accelerate (to ~11× equilibrium rates in the default run; differing weathering sensitivities are compared in Fig. 3). Elevated weathering increases delivery of DIC, TA, and DSi to the oceans (Equations 1 and 2), restoring $CaCO_3$ and SiO_2 oversaturation, and rapid burial of both SiO_2 and $CaCO_3$ (Equations 3 and 4) commences quickly (within tens of thousands of years of deglaciation, although previous modeling [Gernon et al., 2016; Le Hir et al., 2008a] suggests that even a modest supply of alkalinity during SE results in more immediate post-glacial cap carbonate burial, alleviating this apparent discrepancy with immediate cap carbonate deposition inferred from the geologic record [Hoffman et al., 2007]). $CaCO_3$ burial peaks within 20 k.y. of its onset, consistent with rapid initial cap deposition (Shields, 2005; Yang et al., 2017), but also remains elevated for 10^5–10^6 yr, consistent with the longer total cap carbonate depositional durations suggested by paleomagnetic reversal stratigraphy (Trindade et al., 2003).

In the default run, post-SE $CaCO_3$ burial exceeds that of SiO_2 in rate (peaking at ~1.6×10^{14} mol $CaCO_3$/yr versus ~4×10^{13} mol SiO_2/yr) and total excess burial (1.2×10^{20} mol $CaCO_3$ versus 3.3×10^{19} mol SiO_2). But depending on the relative strength of silicate and carbonate weathering feedbacks (both poorly constrained, especially so for the Precambrian), the magnitude and timing of excess $CaCO_3$ versus SiO_2 burial can be shifted. Runs using a strong carbonate weathering feedback and weak Si-weathering generate a rapid and massive cap $CaCO_3$ burial event that dwarfs the burial of SiO_2, which may be distributed over millions of years (Fig. 3). Conversely, strong silicate and weak carbonate

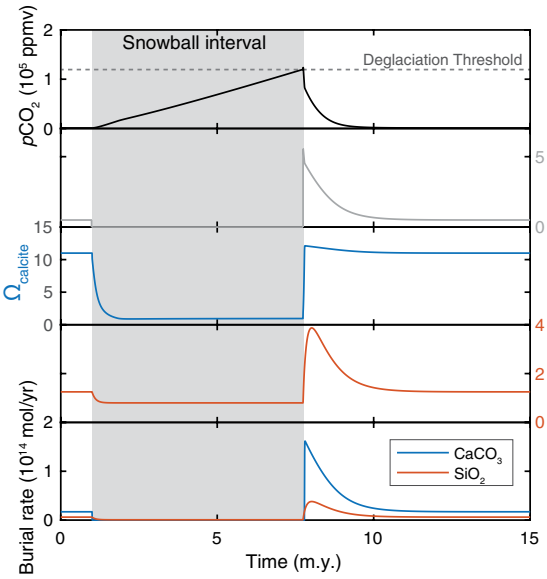

Figure 2. Full snowball Earth simulation in PreCOSCIOUS (PreCambrian Ocean Silica Carbon Inorganic Ocean Underwater Sediment model; see the Data Repository [see footnote 1]). At time t = 1 m.y., snowball forcing is triggered (only external input to model; gray bar indicates snowball interval), which shuts down chemical weathering, allowing CO_2 to accumulate in atmosphere. When pCO_2 reaches deglaciation threshold (0.12 bar), snowball forcing stops, simulating deglaciation. High pCO_2 and temperature immediately following deglaciation results in extremely high carbonate- and silicate-weathering fluxes, which quickly restore carbonate and SiO_2 saturation state, triggering precipitation and burial of $CaCO_3$ and SiO_2. $\Omega_{calcite}$ is the saturation state of calcite; [DSi] is the concentration of dissolved silica; F_{SilW} describes global total silicate-weathering (Equation 1) rate.

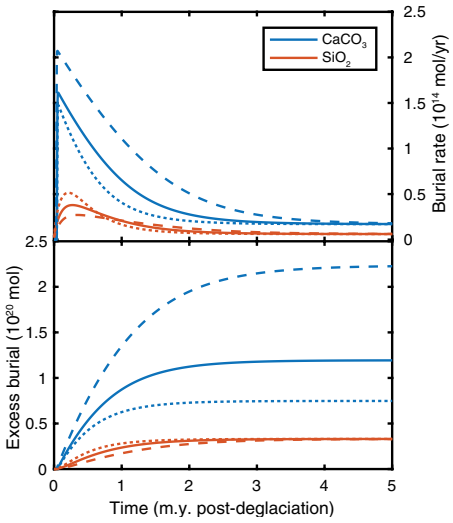

Figure 3. Sensitivity of post-snowball $CaCO_3$ and SiO_2 burial to carbonate and silicate weathering feedback strengths. PreCOSCIOUS (PreCambrian Ocean Silica Carbon Inorganic Ocean Underwater Sediment model; see the Data Repository [see footnote 1]) calculates carbonate and silicate weathering rates individually as functions of pCO_2 with form $F_w = F_{wi}$ $(pCO_2/pCO_{2i})^n$ (see the Data Repository [see footnote 1] for full model description), where pCO_{2i} and F_{wi} are pre-snowball equilibrium pCO_2 and weathering rate, respectively, at which point CO_2 consumption by weathering balances volcanic degassing and input and output fluxes are balanced for all model tracers (Berner et al., 1983; Zeebe, 2012). Exponent n sets strength of each weathering feedback, or how sensitive weathering fluxes are to changes in pCO_2. Standard run (solid lines) uses an n of 0.5 for both carbonate and silicate weathering. Short-dashed lines show model runs using weaker carbonate (n = 0.4) and stronger silicate (n = 0.6) weathering feedbacks, while long-dashed lines use stronger carbonate and weaker silicate weathering. Excess burial is cumulative burial above pre-snowball equilibrium burial rates, starting at point of deglaciation (area under burial-rate curves shown in top panel). Excess $CaCO_3$ burial varies with carbonate weathering feedback strength, but excess SiO_2 burial approaches same total (3.3×10^{19} mol SiO_2) regardless of carbonate or silicate weathering feedback strengths, reflecting mass-balance requirement that total excess silicate weathering equal (in moles) amount of volcanogenic carbon needed to trigger deglaciation (see main text), which is constant across these three simulations.

weathering feedbacks generate SiO_2 and $CaCO_3$ burial of similar rate and mass. Remarkably, the excess $CaCO_3$ burial allowed by the range of weathering feedbacks explored in Figure 3 compares favorably to the observed size of Marinoan cap carbonate deposits globally: a range of 7.5 $\times$ 10^{19} to 2.2 $\times$ 10^{20} mol $CaCO_3$ is equivalent to 15–45 m $CaCO_3$ distributed over the area of the seafloor.

Further sensitivity tests that explore variations in the parameters and processes selected for the favored configuration, including "hard" (no glacial air-sea gas exchange) and "soft" SE forcings, different equilibrium pCO_2 and deglaciation thresholds, and scenarios of syn-glacial carbonate dissolution and $[Ca^{2+}]$ evolution, allow quantitatively different model behavior. However, all model configurations feature rapid (beginning within tens of thousands of years) and massive post-SE burial of SiO_2 and $CaCO_3$ due to the high rates of chemical weathering.

Despite the range of possible $CaCO_3$ burial mass and rate allowed by uncertainty in the weathering feedback, cumulative excess SiO_2 burial is constant across all weathering configurations. This feature (the insensitivity of total SiO_2 burial to weathering feedback strengths) is a simple mass-balance requirement, robust across all model runs in which Si-weathering rate increases in response to elevated pCO_2 (that is to say, any Si-weathering feedback at all). Si-weathering differs from carbonate weathering in that Si-weathering, followed by the subsequent carbonate burial it promotes, actually removes C from the exogenic C cycle (Equation 2 balanced by Equation 3 leads to net removal of CO_2). By contrast, while carbonate weathering balanced by carbonate burial involves a flux of carbon from continents to sediments (and likely plays a crucial role considering the size and extent of cap carbonates), it has no long-term net effect on the ocean-atmosphere carbon budget (Equation 3 is the reverse of Equation 1). The recovery of the C cycle to its pre-perturbation equilibrium involves the removal by Si-weathering of the high atmospheric CO_2 required for deglaciation. Indeed, the total excess SiO_2 burial common to all combinations of weathering strengths (3.3×10^{19} mol SiO_2) is stoichiometrically equivalent (in moles) to the total volcanic CO_2 emitted during the SE interval (volcanic degassing at 5×10^{12} mol CO_2/yr multiplied by a SE duration of 6.7 m.y. gives 3.3×10^{19} mol CO_2). Put another way, the total post-SE excess SiO_2 burial is equal to the weathering-derived DSi that would have been delivered to the oceans during that 6.7 m.y. glacial period, were it not for the weathering shutdown during glaciation.

GEOLOGIC EVIDENCE FOR Si-CYCLE PERTURBATION

Given that Si-weathering during SE deglaciation would deliver ~10^{19} mol of DSi to the ocean that would have to be balanced by burial, does the geologic record provide evidence for elevated SiO_2 burial following proposed SE glacial episodes? The most convincing evidence comes from West Africa (Fig. 4), where Neoproterozoic glacial diamictites in the Volta Basin are overlain by a relatively thin 1–6 m carbonate unit immediately below a much thicker (~30 m) bedded chert (Porter et al., 2004; Trompette et al., 1980). This Marinoan triad of glacial tillite, carbonate, and chert is recognized in sections across the West African craton (extending across millions of square kilometers; Flicoteaux and Trompette, 1998). In Central Africa (Congo Basin), Marinoan cap carbonates are commonly interbedded with chert lenses (Mickala et al., 2014), and chert is ubiquitous in cap dolostone of the Taoudéni Basin of Senegal and Guinea (Shields et al., 2007). In Mongolia, at least two chronostratigraphically distinct Neoproterozoic diamictite–cap carbonate couplets co-occur with chert nodules and beds within the transgressive systems tract (Bold et al., 2016; Macdonald et al., 2009). These "cap cherts" in Africa and Mongolia appear to represent the fate of DSi weathering off the continents in the aftermath of the Marinoan SE.

While those regions show evidence for silica burial in support of our simulations of a massive Si-weathering pulse following deglaciation, cap cherts are clearly not as ubiquitous as Marinoan cap carbonates. This is to be expected, as SiO_2 burial should occur contemporaneously with much more rapid and massive $CaCO_3$ burial (Figs. 2 and 3). Indeed, 3.3×10^{19} mol SiO_2 corresponds to only ~2 m of chert distributed over the seafloor (an order of magnitude smaller than cap carbonates), which, if concentrated by points of riverine input and spatial variations in SiO_2 mineral solubility with temperature and pressure into regions of the ocean, could be accounted for by the ~30-m-thick bedded chert observed above the Marinoan in West Africa. Furthermore, the full extent of post-glacial SiO_2 burial may not be fully recognized, for two reasons: (1) Precambrian burial could also have occurred through the diagenetic silicification of preexisting sediments at the seafloor (Siever, 1992)—in the case of Neoproterozoic deglaciations, the predominately siliciclastic glacial deposits themselves—which may have obscured its recognition; and (2) the coldest parts of the ocean may have been the main locus of SiO_2 burial (due to the temperature effect on SiO_2 solubility), sedimentary records of which have long been lost to subduction.

Further observational constraints on the response of the Si-cycle and SiO_2 burial rate during Neoproterozoic deglaciations could shed

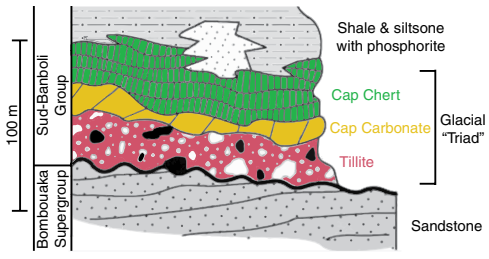

Figure 4. Generalized stratigraphy of West African Neoproterozoic tillite-carbonate-chert triads. In Volta Basin, Neoproterozoic glaciogenic tillite is immediately overlain by thin (1–10 m) cap carbonates and comparatively thicker (~30 m) bedded chert, termed here "cap cherts." Modified from Porter et al. (2004), originally from Trompette et al. (1980).

light on the upper limits of Earth's weathering feedback—a crucial unknown in the carbon cycle, and one that was likely very different before the rise of land plants (Berner, 1998). The strength of that weathering feedback may be relevant to the durations of both SE glaciations and intervening ice-free intervals (Mills et al., 2011). But it is clear that if the SE hypothesis accurately describes Neoproterozoic glacial intervals, the intense weathering following deglaciation (enough to sequester 0.12 bar pCO_2, or ~400,000 Gt C, releasing almost 1×10^6 Gt Si) likely represents the largest perturbation of the C and Si cycles in Earth history.

ACKNOWLEDGMENTS

We thank three anonymous reviewers for their constructive comments, and editor J.T. Parish for her careful attention that improved the manuscript.

REFERENCES CITED

Bao, H., Lyons, J.R., and Zhou, C., 2008, Triple oxygen isotope evidence for elevated CO_2 levels after a Neoproterozoic glaciation: Nature, v. 453, p. 504–506, https://doi.org/10.1038/nature06959.

Berner, R.A., 1998, The carbon cycle and CO_2 over Phanerozoic time—The role of land plants: Philosophical Transactions of the Royal Society of London: Series B, Biological Sciences, v. 353, p. 75–82, https://doi.org/10.1098/rstb.1998.0192.

Berner, R.A., Lasaga, A.C., and Garrels, R.M., 1983, The carbonate-silicate geochemical cycle and its effects on atmospheric carbon dioxide over the past 100 million years: American Journal of Science, v. 283, p. 641–683, https://doi.org/10.2475/ajs.283.7.641.

Bold, U., Smith, E.F., Rooney, A.D., Bowring, S.A., Buchwaldt, R., Dudás, F.Ö., Ramezani, J., Crowley, J.L., Schrag, D.P., and Macdonald, F.A., 2016, Neoproterozoic stratigraphy of the Zavkhan terrane of Mongolia: The backbone for Cryogenian and early Ediacaran chemostratigraphic records: American Journal of Science, v. 316, p. 1–63, https://doi.org/10.2475/01.2016.01.

Caldeira, K., and Kasting, J.F., 1992, Susceptibility of the early Earth to irreversible glaciation caused by carbon dioxide clouds: Nature, v. 359, p. 226–228, https://doi.org/10.1038/359226a0.

Evans, D.A.D., and Raub, T.D., 2011, Neoproterozoic glacial palaeolatitudes: A global update, *in* Arnaud, E., et al., eds., The Geological Record of Neoproterozoic Glaciations: Geological Society of London Memoir 36, p. 93–112, https://doi.org/10.1144/M36.7.

Flicoteaux, R., and Trompette, R., 1998, Cratonic and foreland Early Cambrian phosphorites of West Africa: Palaeoceanographical and climatical contexts: Palaeogeography, Palaeoclimatology, Palaeoecology, v. 139, p. 107–120, https://doi.org/10.1016/S0031-0182(97)00141-7.

Gernon, T.M., Hincks, T.K., Tyrrell, T., Rohling, E.J., and Palmer, M.R., 2016, Snowball Earth ocean chemistry driven by extensive ridge volcanism during Rodinia breakup: Nature Geoscience, v. 9, p. 242–248, https://doi.org/10.1038/ngeo2632.

Higgins, J.A., and Schrag, D.P., 2003, Aftermath of a snowball Earth: Geochemistry Geophysics Geosystems, v. 4, 1028, https://doi.org/10.1029/2002GC000403.

Hoffman, P.F., and Schrag, D.P., 2002, The snowball Earth hypothesis: Testing the limits of global change: Terra Nova, v. 14, p. 129–155, https://doi.org/10.1046/j.1365-3121.2002.00408.x.

Hoffman, P.F., Kaufman, A.J., Halverson, G.P., and Schrag, D.P., 1998, A Neoproterozoic snowball Earth: Science, v. 281, p. 1342–1346, https://doi.org/10.1126/science.281.5381.1342.

Hoffman, P.F., Halverson, G.P., Domack, E.W., Husson, J.M., Higgins, J.A., and Schrag, D.P., 2007, Are basal Ediacaran (635 Ma) post-glacial "cap dolostones" diachronous?: Earth and Planetary Science Letters, v. 258, p. 114–131, https://doi.org/10.1016/j.epsl.2007.03.032.

Hoffman, P.F., et al., 2017, Snowball Earth climate dynamics and Cryogenian geology-geobiology: Science Advances, v. 3, e1600983, https://doi.org/10.1126/sciadv.1600983.

Huang, K.-J., Teng, F.-Z., Shen, B., Xiao, S., Lang, X., Ma, H.-R., Fu, Y., and Peng, Y., 2016, Episode of intense chemical weathering during the termination of the 635 Ma Marinoan glaciation: Proceedings of the National Academy of Sciences of the United States of America, v. 113, p. 14,904–14,909, https://doi.org/10.1073/pnas.1607712113.

James, N.P., Narbonne, G.M., and Kyser, T.K., 2001, Late Neoproterozoic cap carbonates: Mackenzie Mountains, northwestern Canada: Precipitation and global glacial meltdown: Canadian Journal of Earth Sciences, v. 38, p. 1229–1262, https://doi.org/10.1139/e01-046.

Kasemann, S.A., von Strandmann, P.A.P., Prave, A.R., Fallick, A.E., Elliott, T., and Hoffmann, K.-H., 2014, Continental weathering following a Cryogenian glaciation: Evidence from calcium and magnesium isotopes: Earth and Planetary Science Letters, v. 396, p. 66–77, https://doi.org/10.1016/j.epsl.2014.03.048.

Kirschvink, J.L., 1992, Late Proterozoic low-latitude global glaciation: The snowball Earth, *in* Schopf, J.W., and Klein, C., eds., The Proterozoic Biosphere : A Multidisciplinary Study: New York, Cambridge University Press, p. 51-52.

Le Hir, G., Goddéris, Y., Donnadieu, Y., and Ramstein, G., 2008a, A geochemical modelling study of the evolution of the chemical composition of seawater linked to a "snowball" glaciation: Biogeosciences, v. 5, p. 253–267, https://doi.org/10.5194/bg-5-253-2008.

Le Hir, G., Ramstein, G., Donnadieu, Y., and Goddéris, Y., 2008b, Scenario for the evolution of atmospheric pCO_2 during a snowball Earth: Geology, v. 36, p. 47–50, https://doi.org/10.1130/G24124A.1.

Macdonald, F.A., Jones, D.S., and Schrag, D.P., 2009, Stratigraphic and tectonic implications of a newly discovered glacial diamictite–cap carbonate couplet in southwestern Mongolia: Geology, v. 37, p. 123–126, https://doi.org/10.1130/G24797A.1.

Maliva, R.G., Knoll, A.H., and Siever, R., 1989, Secular change in chert distribution: A reflection of evolving biological participation in the silica cycle: Palaios, v. 4, p. 519–532, https://doi.org/10.2307/3514743.

Mickala, O.-R., Vidal, L., Boudzoumou, F., Affaton, P., Vandamme, D., Borschneck, D., Mounguengui, M.M., Fournier, F., Nganga, D.M.M., and Miche, H., 2014, Geochemical characterization of the Marinoan "Cap Carbonate" of the Niari-Nyanga Basin (Central Africa): Precambrian Research, v. 255, p. 367–380, https://doi.org/10.1016/j.precamres.2014.10.001.

Mills, B., Watson, A.J., Goldblatt, C., Boyle, R., and Lenton, T.M., 2011, Timing of Neoproterozoic glaciations linked to transport-limited global weathering: Nature Geoscience, v. 4, p. 861–864, https://doi.org/10.1038/ngeo1305.

Penman, D.E., 2016, Silicate weathering and North Atlantic silica burial during the Paleocene-Eocene Thermal Maximum: Geology, v. 44, p. 731–734, https://doi.org/10.1130/G37704.1.

Pierrehumbert, R.T., 2004, High levels of atmospheric carbon dioxide necessary for the termination of global glaciation: Nature, v. 429, p. 646–649, https://doi.org/10.1038/nature02640.

Porter, S.M., Knoll, A.H., and Affaton, P., 2004, Chemostratigraphy of Neoproterozoic cap carbonates from the Volta basin, West Africa: Precambrian Research, v. 130, p. 99–112, https://doi.org/10.1016/j.precamres.2003.10.015.

Rooney, A.D., Macdonald, F.A., Strauss, J.V., Dudás, F.Ö., Hallmann, C., and Selby, D., 2014, Re-Os geochronology and coupled Os-Sr isotope constraints on the Sturtian snowball Earth: Proceedings of the National Academy of Sciences of the United States of America, v. 111, p. 51–56, https://doi.org/10.1073/pnas.1317266110.

Shields, G.A., 2005, Neoproterozoic cap carbonates: A critical appraisal of existing models and the *plumeworld* hypothesis: Terra Nova, v. 17, p. 299–310, https://doi.org/10.1111/j.1365-3121.2005.00638.x.

Shields, G.A., Deynoux, M., Culver, S.J., Brasier, M.D., Affaton, P., and Vandamme, D., 2007, Neoproterozoic glaciomarine and cap dolostone facies of the southwestern Taoudéni Basin (Walidiala Valley, Senegal/Guinea, NW Africa): Comptes Rendus Geoscience, v. 339, p. 186–199, https://doi.org/10.1016/j.crte.2006.10.002.

Siever, R., 1992, The silica cycle in the Precambrian: Geochimica et Cosmochimica Acta, v. 56,. 3265–3272, https://doi.org/10.1016/0016-7037(92)90303-Z.

Trindade, R.I.F., Font, E., D'Agrella-Filho, M.S., Nogueira, A.C.R., and Riccomini, C., 2003, Low-latitude and multiple geomagnetic reversals in the Neoproterozoic Puga cap carbonate, Amazon craton: Terra Nova, v. 15, p. 441–446, https://doi.org/10.1046/j.1365-3121.2003.00510.x.

Trompette, R., Affaton, P., Joulia, F., and Marchand, J., 1980, Stratigraphic and structural controls of late Precambrian phosphate deposits of the northern Volta Basin in Upper Volta, Niger, and Benin, West Africa: Economic Geology and the Bulletin of the Society of Economic Geologists, v. 75, p. 62–70, https://doi.org/10.2113/gsecongeo.75.1.62.

Urey, H.C., 1952, On the early chemical history of the earth and the origin of life: Proceedings of the National Academy of Sciences of the United States of America, v. 38, p. 351–363, https://doi.org/10.1073/pnas.38.4.351.

Walker, J.C.G., and Kasting, J.F., 1992, Effects of fuel and forest conservation on future levels of atmospheric carbon dioxide: Palaeogeography, Palaeoclimatology, Palaeoecology, v. 97, p. 151–189, https://doi.org/10.1016/0031-0182(92)90207-L.

Walker, J.C.G., Hays, P.B., and Kasting, J.F., 1981, A negative feedback mechanism for the long-term stabilization of Earth's surface temperature: Journal of Geophysical Research, v. 86, p. 9776–9782, https://doi.org/10.1029/JC086iC10p09776.

Yang, J., Jansen, M.F., Macdonald, F.A., and Abbot, D.S., 2017, Persistence of a freshwater surface ocean after a snowball Earth: Geology, v. 45, p. 615–618, https://doi.org/10.1130/G38920.1.

Zeebe, R.E., 2012, LOSCAR: Long-term Ocean-atmosphere Sediment CArbon Reservoir Model v2.0.4: Geoscientific Model Development, v. 5, p. 149–166, https://doi.org/10.5194/gmd-5-149-2012.

Zeebe, R.E., and Westbroek, P., 2003, A simple model for the $CaCO_3$ saturation state of the ocean: The "Strangelove", the "Neritan", and the "Cretan" Ocean: Geochemistry Geophysics Geosystems, v. 4, https://doi.org/10.1029/2003GC000538.

Printed in USA